

ISLANDING DETECTION OF INVERTER-BASED DISTRIBUTED GENERATION USING DC-LINK VOLTAGE FUZZY CONTROL

RAJANI KOKKONDA

Pg Scholar, Vaagdevi College Of Engineering.

Dr. K. PRAKASH

Principal, Vaagdevi College Of Engineering

ABSTRACT--This paper proposes islanding detection if inverter based distributed generation (DG) using DC-link voltage fuzzy control. A new method for islanding detection of inverter-based distributed generation (DG). In, the islanding is defined as a condition in which a portion of an electric power system is solely energized and separated from the rest of the electric power system. The main idea of this paper is to change the dc-link voltage considering the PCC voltage changes during islanding condition. A simple islanding detection scheme has been designed based on this idea. The proposed method has been studied under multiple-DG operation modes with using fuzzy logic controller. This proposed method has a small non-detection zone. Also, this method is capable of detecting islanding accurately within the minimum standard time. The simulations results, carried out by MATLAB/Simulink.

I. INTRODUCTION

Integrations of distributed generations (DGs) in the distribution network is expected to play an increasingly important role in the electric power system infrastructure and market. As more DG systems become part of the power grid, there is an increased safety hazard for personnel and an increased risk of damage to the power system. Despite the favorable aspects grid-connected DGs can provide to the distribution system, a critical demanding concern is islanding detection and prevention. Islanding is a condition where the DG supplies power and is not under the direct control of the utility.

Islanding detection techniques may be classified as passive or active. Passive techniques use information available at the DG side to determine whether the DG system is isolated from the grid. The advantage of passive techniques is that the implementation does not have an impact on the normal operation of the DG system. Active techniques introduce an external perturbation at the output of the inverter. These tend

to have a faster response and a smaller non-detection zone compared to passive approaches. However, the power quality (PQ) of the inverter can be degraded by the perturbation. In this case, the amount of frequency or voltage deviation will not be sufficient to trigger the islanding detection system. Several passive islanding detection methods are available, such as under voltage/overvoltage; under frequency/over frequency; rate of change of active power; rate of change of frequency (ROCOF) rate of change of frequency over power, voltage and power factor changes, phase jump detection, and voltage unbalance and total harmonic distortion. Passive islanding detection methods suffer from large non-detection zones (NDZs). NDZs are defined as a loading condition for which an islanding detection method would fail to operate in a timely manner.

Active techniques have been designed to force DG to be unstable in islanding mode and interact with the operation of the power system directly. The main advantage of active techniques over passive techniques is their small. Active methods include slide-mode frequency shift, active frequency drift or frequency bias, Sandia frequency shift, and harmonic distortion base. Active methods have a smaller NDZ and can degrade the PQ of the power system. Communication-based methods do not have any NDZ, but they are more expensive than the former methods.

This paper presents a new islanding detection method, which has the advantages of active and passive islanding methods, small NDZ, and good accuracy. The control strategy of the voltage-source inverter has been designed to operate at unity power factor. Also, the dc side has been modeled by a controllable dc voltage source. The main idea of this paper is to change the dc-link voltage considering the PCC voltage changes during the islanding condition. A simple and easy-to-implement method, such as

The reactive power controller, shown in Fig. 2,

frequency component in the output voltage determines the amplitude-modulation ratio (m_a), by the following equation: — (8)

$$\text{—————(9)}$$

Where V_{control} is the peak amplitude of the control signal and the V_{tri} is the amplitude of the triangular signal. Therefore, the line-to-line rms voltage at the fundamental frequency can be written, as follows:

$$\text{—————} \quad \text{—————} \quad (10)$$

Now, the following equations can be written for V_{dt} and V_{qt} :

$$(11)$$

$$(12)$$

Where Φ is the angle by which the inverter voltage vector leads the line voltage vector. In a lossless inverter, the instantaneous power at the ac and dc terminals of the inverter is equal. This power balance can be written, as follows:

$$\text{—————} \quad (13)$$

At the dc link, we have

$$\text{—————} \quad (14)$$

By using (4) and (11)–(14), the following state equations can be written

$$\text{—————} \quad \text{—————} \quad \text{—————} \quad \text{—————} \quad (15)$$

PROPOSED ISLANDING DETECTION METHOD:

The acceptable voltage deviation is in the range of 88% to 110% of the nominal voltage. Any voltage deviation in this range should not be detected and the corresponding load condition would be considered within the NDZ. It is assumed that DG has been designed to operate at a constant dc voltage of 900 V. In this section, a new analytical formulation is derived by the linearization of system state equations. Then, a new V_{dc} - V_{pcc} characteristic of DG will be explained, and the performance of this method will be evaluated.

To measure the impact of deviation of m_a on dc-link voltage, Φ has been kept constant and only m_a has been considered as a variable. As a result, (15) is a nonlinear equation. However, for a small perturbation around the equilibrium point m_a , the following linear set of equations can be obtained, where subscript 0 denotes steady-state values, as shown in (16) at the bottom of the page.

The inverter steady-state model can be obtained from the dynamic model by setting the derivative terms equal to zero. After transformation from to the reference frame, the voltages and the currents become dc quantities. Therefore, substituting

$$\text{—————} \quad \text{—————} \quad \text{—————} \quad \text{—————} \quad (16)$$

and simplification of the steady-state model resulted in the following equation:

$$\text{—————} = \text{—————} \quad (17)$$

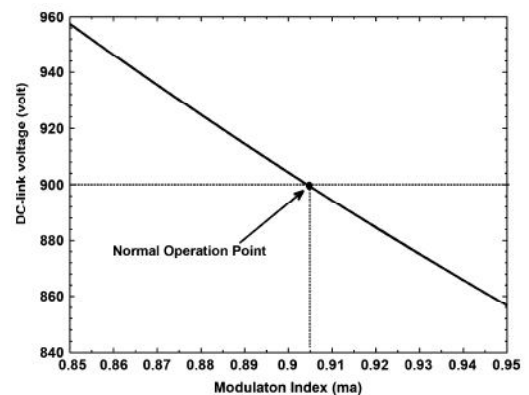


Fig. 3. Steady-state variations of V_{dc} versus m_a (with $L_f = 2.1$ mH, $\Phi = 377$ rad/s, $R_f = 0.00145\Omega$, $\Phi = 20^\circ$ and $V_{pcc} = 1$ p.u). measured quantities are real numbers (crisp). The FLC takes two inputs, i.e., the error and the rate of change of

By solving (17) for i_{dt}, i_{qt} and V_{dc} , we have

$$\text{—————} \quad (18)$$

$$\text{—————} \quad (19)$$

$$\text{—————} \quad (20)$$

Considering (18) and (19), it is obvious that I_{dt} and I_{qt} do not depend on the modulation index (m_a). For the given system, the variations of V_{dc} versus m_a can be determined by using (20). By considering it as a constant value, (20) becomes a hyperbolic equation. But the part $m_a < 0$ is not acceptable and just the part $0 < m_a < 1$ is the dominant. By scaling m_a between 0.8 and 1, it can be seen that the deviation of m_a versus V_{dc} is linear and usually the normal operating point of the inverter is in this range. The V_{dc} - m_a curve of this range has been shown in Fig. 3. Considering (10), we have

$$\text{—————} \quad (21)$$

In steady-state condition, (10) can be written as follows:

$$\text{—————} \quad (22)$$

By combining (21) and (22), we have

$$\text{—————} \quad (23)$$

Considering (20) and Fig. 3, it is obvious that the deviation of m_a around the operating point does not have any major impact on drifting of the dc-link voltage. Therefore, the modulation index can be assumed to be constant (i.e., $m_a = m_{a0}$). Then, (23) can be written as follows:

$$\text{—————} \quad (24)$$

III. FUZZY LOGIC CONTROLLER

FLC contains three basic parts: Fuzzification, Base rule, and Defuzzification. FLC has two inputs which are: error and the change in error, and one output. The Fuzzy Controller structure is represented in figure 4. The role of each block is the following:

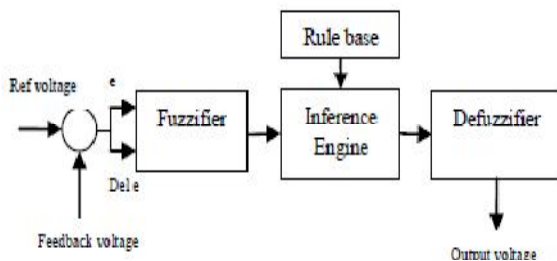


Fig 4: The general structure of Fuzzy Logic Controller

Fuzzifier converts a numerical variable into a linguistic label. In a closed loop control system, the error (e) between the reference voltage and the output voltage and the rate of change of error (Δe) can be labeled as zero (ZE), positive small (PS), negative small (NS), etc. In the real world, m

error. Based on these inputs, The FLC takes an intelligent decision on the amount of field voltage to be applied which is taken as the output and applied directly to the field winding of generator. Triangular membership functions were used for the controller.

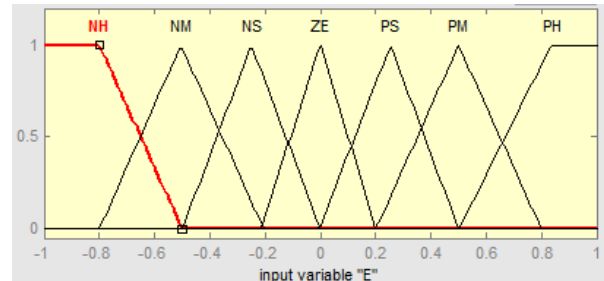


Figure.5 Membership function of error

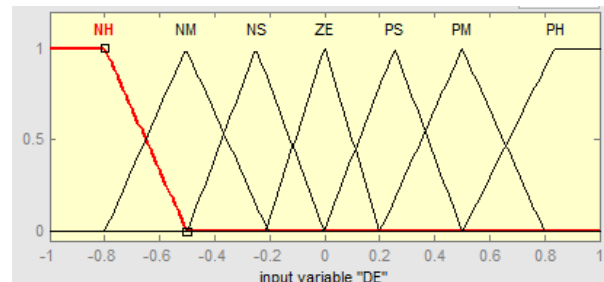


Figure.6 Membership function of change in error

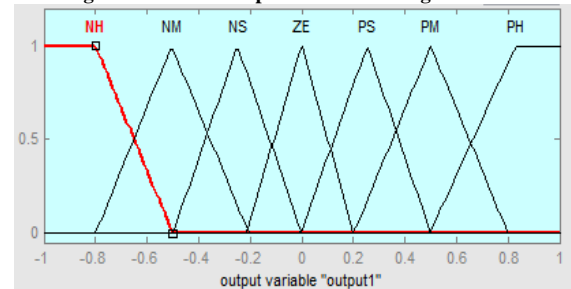


Figure 7. Membership function of output

Rule base stores the data that defines the input and the output fuzzy sets, as well as the fuzzy rules that describe the control strategy. Mamdani method is used in this paper. Seven membership functions were used leading to 49 rules in the rule base.

Table 1: Rule base for fuzzy controller

	NH	NM	NS	ZE	PS	PM	PH
NH	PH						
NM	PM						
NS	PS						
ZE	PS	PS	ZE	ZE	ZE	PS	PS
PS							
PM							

occurrence of islanding).

PH							
----	----	----	----	----	----	----	----

Inference engine applies the fuzzy rules to the input fuzzy variables to obtain the output values. Defuzzifier achieves output signals based on the output fuzzy sets obtained as the result of fuzzy reasoning. Centroid defuzzifier is used here

IV. SIMULATION RESULTS

In this section, the test system shown in Fig. 1 has been simulated by MATLAB/Simulink. The system, DG, and load parameters are listed in Table II. The parameter has been set to 0 MVar. The Islanding detection method has been tested for load with a quality factor () of 1.77. The proposed islanding detection method has been also tested for various loading conditions [3].

TABLE II
SYSTEM, DG, AND LOAD PARAMETERS

Grid and inverter parameters	
DG output power	100 Kw
Switching Frequency	8000 Hz
Input DC Voltage	900 V
Voltage (L-L)	480 V
Frequency	60 Hz
Grid resistance	0.02 Ω
Grid Inductance	0.3 mH
Filter Inductance	2.1 mH
DG Controller parameters	
Q Control	, = 0.01
	, = 9.78
PI control	, = 1250
Load parameters	
R	2.304 Ω
L	0.00345 H
C	2037 F

The active load power is adjusted to set the inverter at 25%, 50%, 100%, and 125% of the rated output power of the inverter. The reactive power has been adjusted between 95% and 105% of the balanced condition (unity power factor loading) in 1% steps [3]. The islanding detection scheme is tested based on the procedure presented in [3]. But all results have not been presented in this section. The DG interface has been equipped with the characteristic given in (31) and islanding has occurred at $t = 0.8$ s. The first simulation result using the proposed method is shown in Fig. 8. This figure shows the voltage at the PCC during an islanding condition, for the active load power adjusted at 50%, 100%, and 125% of its rated output power. The reactive power has been adjusted at 100% of the balanced condition. As can be seen in Fig. 9, the PCC voltage exceeds the OVP/UVF thresholds in less than 100 ms (after the

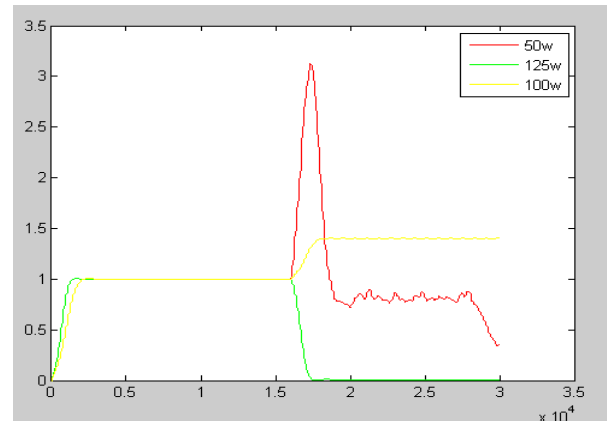


Fig. 8. PCC voltage using the proposed characteristic for different loads.

Fig. 9 shows the voltage at the PCC during an islanding condition, for the following cases [4]:

Case 1) The load has been adjusted to operate at 100% of rated active power with 101% reactive power in the balanced condition.

Case 2) The load has been adjusted at 100% of the rated active power with 100% reactive power.

Case 3) The load has been adjusted at 100% of its rated active power with 99% reactive power.

Table III lists the load parameters. It can be seen in Fig. 9 that the operation of the DG unit is stable as long as it is connected to the grid. After islanding instant ($t = 0.8$ s), the DG loses its stable operation, and the PCC voltage exceeds the OVP/UVF threshold values in less than 110 ms.

B. Effect of Load Switching:

The proposed islanding detection method has been tested for load switching in the grid-connected operation mode. In parallel with the old load, which has been presented in Fig. 1, the new load has been switched at $t = 0.5$ s and disconnected at $t = 1$ s.

Three cases have been simulated in this test. In all cases, the load apparent power is equal to 100 kVA but the power factor is 0.8 lead, 1.0 and 0.8 lag. The simulation results that include the PCC voltage and frequency, and the DG active and reactive power outputs for three different loading conditions have been presented in Fig. 10. The voltage and frequency variations can be seen when the load is switched on and off. For simulated cases, the voltage and frequency variations are within the standard values.

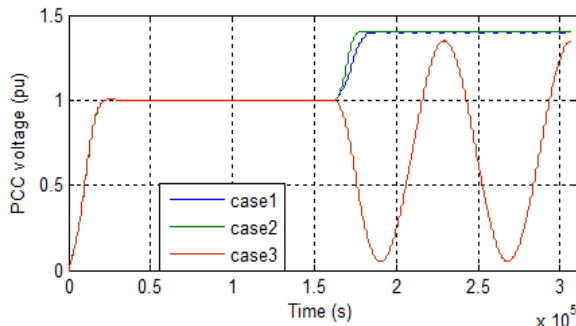


Fig.9. PCC voltage with proposed characteristic for three cases.

It is obvious that the proposed method does not interfere with the power system operation during normal conditions.

**TABLE III
LOAD PARAMETERS FOR UL 1741 TESTS**

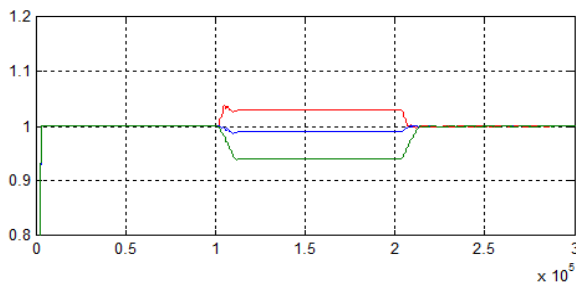
C. Effect of Load Quality Factor:

The IEEE Standard 929 proposes the use of $\cos\phi$ for tests. Yet, recent standards (IEEE 1547.1) propose testing islanding with loads having a quality factor of 1 [30]. The UL 1741 test specifies that an islanding detection method must succeed in detecting the islanding phenomenon within

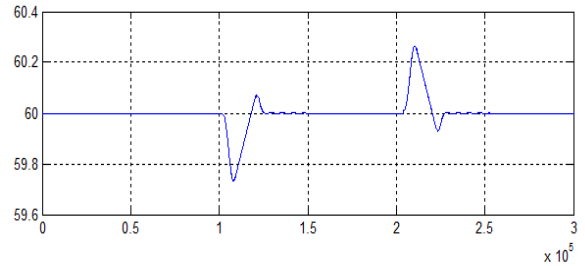
P%	Q%	R(Ω)	L(H)	C(F)
50	100	4.603	0.00345	2037
125	100	1.841	0.00345	2037
100	99	2.304	0.003488	2037
100	100	2.304	0.00345	2037
100	101	2.304	0.003419	2037

2 s for RLC loads

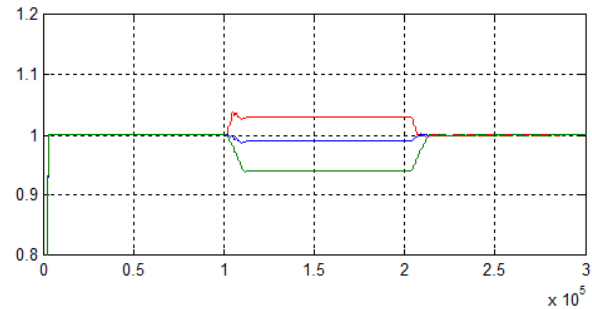
with $\cos\phi = 1.8$ [4]. For the system shown in Fig. 1, $\cos\phi$ has changed in the range of 0.5 to 4.2 by adjusting the load inductance and capacitance according to Table IV.



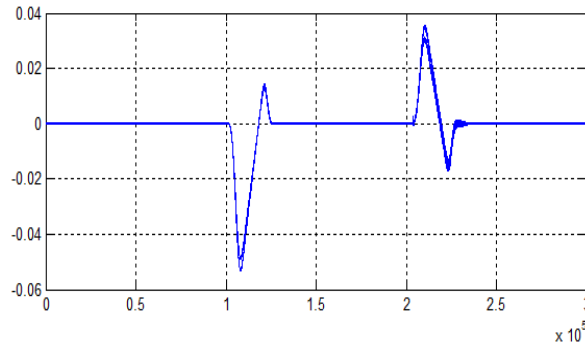
(a)



(b)



(c)



(d)

Fig.10. System response during load switching. (a) PCC voltage. (b) PCC frequency. (c) Inverter active power. (d) Inverter reactive power.

**TABLE IV
LOAD PARAMETERS FOR DIFFERENT**

Q%	R(Ω)	L(H)	C(F)
0.5	2.304	0.0122	575.4
1	2.304	0.0061	1150
1.77	2.304	0.00345	2037
2.12	2.304	0.00288	2439
3	2.304	0.00203	3452
4.2	2.304	0.00145	4833.5

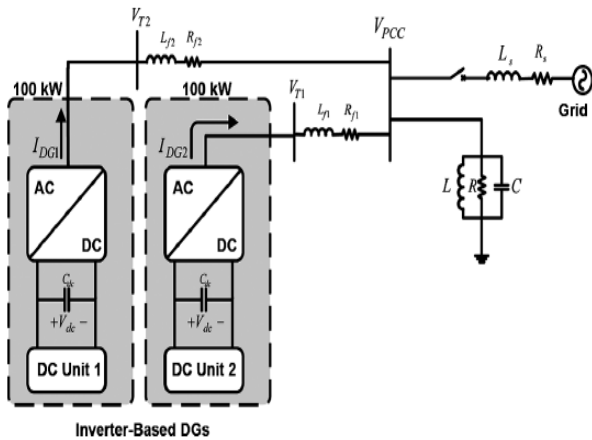


Fig.12. Schematic diagram of the two-DG system.

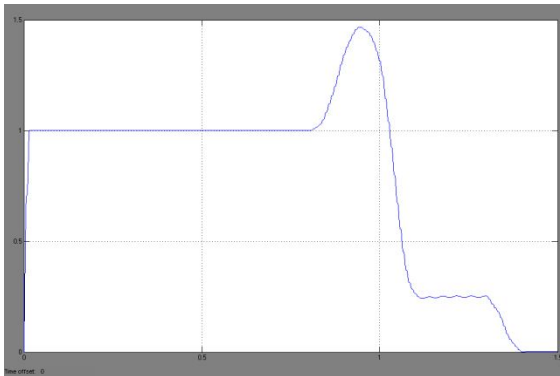


Fig.13. PCC voltage for the multiple-DG operation mode.

CONCLUSION

This paper shows proposes islanding detection if inverter based distributed generation (DG) using DC-link voltage fuzzy control. A new method for islanding detection of an inverter-based DG unit by using the V_{dc} - V_{pcc} characteristic. The V_{dc} - V_{pcc} characteristic has been chosen so that the DG maintains its stable operation in grid-connected and islanding condition modes. Applying the proposed V_{dc} - V_{pcc} characteristic to the DG results in a simple islanding detection method, which can be similar to OVP/UVP protections. The simulation results show the effectiveness of the new islanding detection method for different operating conditions. In addition, it has been shown that this method does not distort any voltage or current waveforms by injecting perturbations and, thus, it has high performance from a PQ point of view. This method is also capable of detecting islanding conditions accurately within the minimum standard time.

REFERENCES



- [1] C. Ma, Z. Lu, W. H. Tang, Q. H. Wu, and J. Fitch, "An agent brokering based scheme for anti-islanding protection of distributed generation," in Proc. Power Energy Soc. Gen. Meeting, Calgary, AB, Canada, 2009, pp. 1–8.
- [2] IEEE Standard for Interconnecting Distributed Resources With Electric Power Systems, IEEE Std. 1547-2003, Jul. 2003.
- [3] Static Inverter and Charge Controllers for Use in Photovoltaic Systems Standard UL, Northbrook, IL: Underwriters Laboratories, Inc., 2001.
- [4] H. H. Zeineldin, "A Q-F droop curve for facilitating Islanding detection of inverter-based distributed generation," IEEE Trans. Power Electron., vol. 24, no. 3, pp. 665–673, Mar. 2009.
- [5] H. H. Zeineldin and J. L. Kirtley, "A simple technique for Islanding detection with negligible non-detection zone," IEEE Trans Power Del., vol. 24, no. 2, pp. 779–786, Apr. 2009.
- [6] K. Tunlasakun, K. Kirtikara, S. Thepa, and V. Monyakul, "CPLD based Islanding detection for mini grid connected inverter in renewable energy," in Proc. IEEE TENCON Conf., Nov. 2004, vol. 4, pp. 175–178.
- [7] W. Freitas, W. Xu, C. M. Affonso, and Z. Huang, "Comparative analysis between ROCOF and vector surge relays for distributed generation applications," IEEE Trans. Power Del., vol. 20, no. 2, pt. 2, pp. 1315–1324, Apr. 2005.
- [8] F. De mango, M. Liserre, and A. D. Aquila, "Overview of Anti Islanding Algorithms for PV Systems. Part II: Active Methods," in Proc. IEEE Power Electronics and Motion Control Conf., Jan. 2007, pp. 1884–1889.
- [9] M. A. Reefer, O. Usta, and G. Fielding, "Protection against loss of utility grid supply for a dispersed storage and generation unit," IEEE Trans. Power Del., vol. 8, no. 3, pp. 948–954, Jul. 1993.
- [10] J. C. M. Vieira, W. Freitas, W. Xu, and A. Morelato, "Efficient coordination of ROCOF and frequency relays for distributed generation protection by using the application region," IEEE Trans. Power Del., vol. 21, no. 4, pp. 1878–1884, Oct. 2006.
- [11] J. P. Moore, J. H. Allmeling, and A. T. Johns, "Frequency relaying based on instantaneous frequency measurement (Power Systems)," IEEE Trans. Power Del., vol. 11, no. 4, pp. 1737–1742, Oct. 1996.
- [12] H. Shyh-Jier and P. Fu-Sheng, "A new approach to Islanding detection of dispersed generators with self-commutated static power converters," IEEE Trans. Power Del., vol. 15, no. 2, pp. 500–507, Apr. 2000.